

Model - Sensor – Information Technology Integration for Machine Tools

Robert B. Jerard

Barry K. Fussell, Bennett Desfosses, Min Xu

Bryan Javorek, Yanjun Cui, Jeffrey Nichols, Raed Hassan, Chris Suprock

Department of Mechanical Engineering

University of New Hampshire, Durham, NH 03824

Donald Esterling

VeritasCNC LLC

Carboro, NC 27510

Abstract: This paper describes recent research progress at the University of New Hampshire in the area of CNC machining. In this work, models of the machining process are integrated with sensor data to improve and monitor the machining processes. This paper summarizes recent progress in model calibration methods, sensor development, model accuracy, tool condition monitoring and information technology for machine tools. We describe a system that can estimate tool wear using the coefficients of a tangential cutting force model. The model coefficients are estimated by online measurement of spindle motor power.

Key Words: Tool wear, tool condition monitoring, spindle motor power, XML, Information Technology

1. Introduction: There has been considerable discussion recently about the development of “smart” machine tools. The definition of a smart machine is still ill-defined, but it is possible to draw parallels with human intelligence. A truly intelligent machine should display some of the same characteristics:

- Adaptation to changing conditions, i.e. the ability to learn from experience and use different processes in the future.
- Integration of sensory input with stored models. Our eyes, ears etc. provide input which is interpreted based on a stored world model.
- Extensive information processing capability.
- A sophisticated language for sharing and storing knowledge. The progress of civilization is based on human language.

There is a tremendous gap between current machine tool technology and these qualities. Presently, machine tools are position servos commanded by a primitive language (G codes) that was developed over fifty years ago in the era of paper tape, long before the ubiquitous computing power of today. Machine tool architecture is long overdue for an extensive overhaul.

A primary focus of our current research is the integration of our machining models into a NC machine open architecture controller (OAC). The models can be used in conjunction with sensor data to perform on-line calibration. A summary of some of our more important contributions is as follows.

1.1 NCML – A New Language for Representation of Machining Process Plans:

Our common interface language is “NCML” a variation of XML for NC described in detail in our publications [Jerard 2006ab]. The key elements of NCML is a “macro” description of machining process plans including XML representations of the workpiece, machining features necessary to transform the workpiece into the desired finished part, and required tolerances and tooling description. Our current research focus is to extend NCML to the representation of machine tool sensor data for purposes of data analysis and archiving.

1.2 Cutting Force Model Calibration: Our force models include both conventional and edge effect contributions [Altintas 2000]. Proper calibration is key to the accuracy of these models. Conventional calibration is cumbersome and may not be reliable if

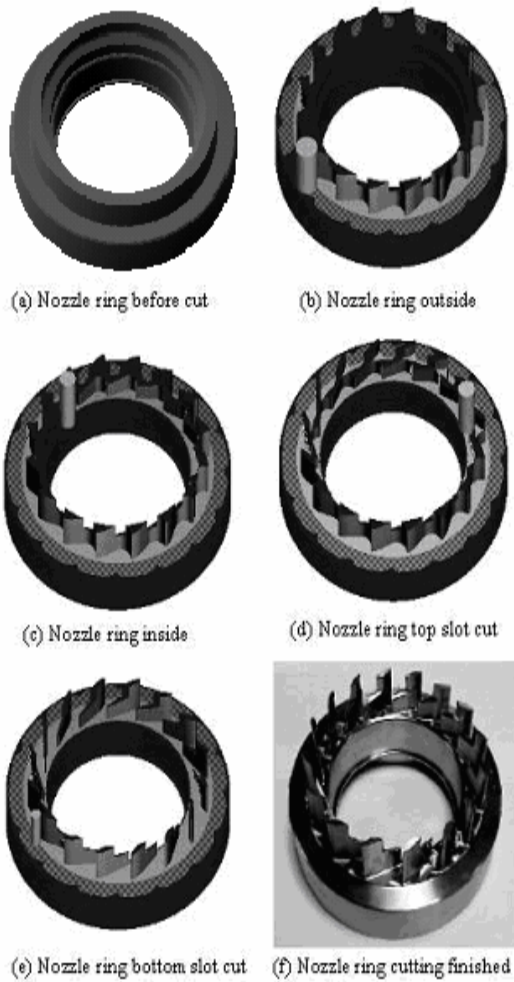


Figure 1 – Nozzle ring test case

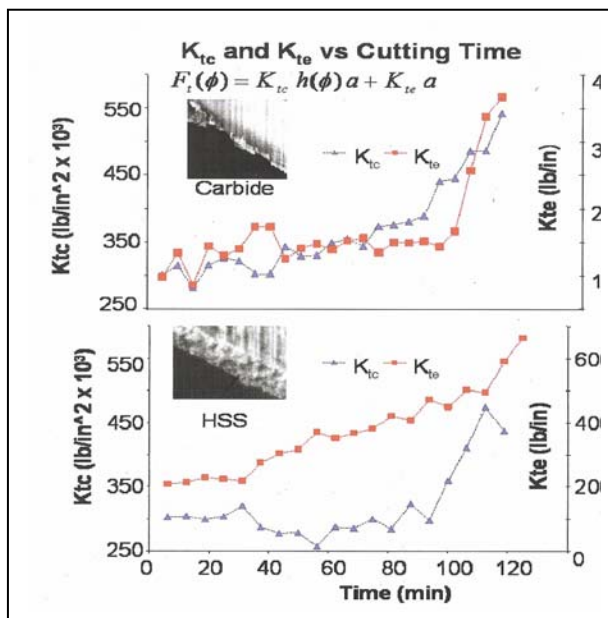


Figure 2 Model parameters are calculated during machining, providing an indication of tool wear.

generalized for nominally the same part material and tooling. Hence it is critical that model parameters be obtained for particular tool/material combinations for acceptable accuracy. We are developing non-invasive on-line calibration methods using spindle motor power information – available from an inexpensive power sensor. [Jerard 05, Schuyler 05].

1.3 Toolpath Planning and Optimization: An industrial partner (TurboCam) supplied us with tooling and stock with a “best practice” part program developed by skilled, experienced programmers for a production part (10,000/month) as shown in **Figure 1**. Our program reduced peak forces by 40% (eliminating a broken tool issue they were experiencing) simultaneously reducing production time by 7%.

1.4 Tool Runout: Runout can currently be measured with an inexpensive manual dial indicator or an expensive, automated laser system. We have investigated the use of a contact microphone as a simple, non-invasive source of high bandwidth data such as needed for dynamic (rotating spindle) runout measurement. Our results demonstrate that we can automatically measure runout by analyzing the vibration signals from an inexpensive contact microphone in lieu of a high bandwidth Kistler force dynamometer. [Jacobson 2006]

1.5 Tool Wear: We have demonstrated that the conventional cutting energy from shearing can be relatively independent of progressive (e.g. flank) tool wear while the edge effect cutting energy tracks well with that wear. This is particularly apparent for HSS tooling, less so but still valid for carbide tooling – each with distinctive wear mechanisms. However, somewhat prior to failure, the conventional cutting energy increases rapidly as shown in **Figure 2**. Together they provide valuable feedback on the tool condition. As the tool wears, tool forces increase often leading to tool or tooth breakage. Industry has consistently asked for a monitoring system that will warn them of failure before the event. The cutting energies are monitored non-invasively and in-process by using spindle motor power data combined with our process models [Jerard 2006a, Xu 2006ab, Xu 2007].

2. Cutting Force Models

2.1 Tangential Force Model: The cutting force vector consists of radial, tangential and longitudinal components. The average tangential force for an end mill cut, regardless of the helix angle, can be shown to be [Altintas 2000]:

$$F_{t_{avg}} = K_{tc} h_{avg} a + K_{te} a \quad (1)$$

where K_{TC} is the cutting coefficient in N/mm^2 , K_{TE} is the edge coefficient in N/mm , h_{avg} is the average chip thickness and a is the axial depth of cut. Nomenclature is illustrated in **Figure 3**.

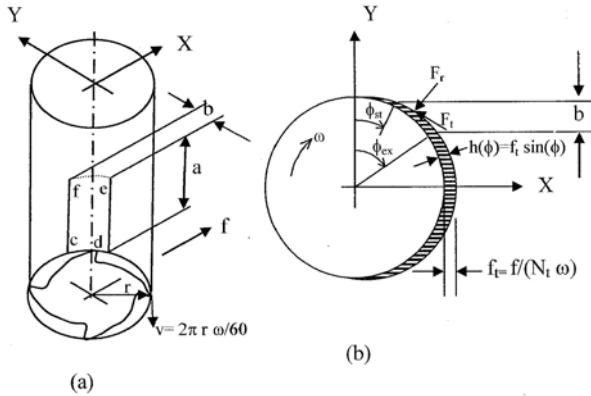


Figure 3 Model nomenclature

The average power required for the cut can be derived by energy principles as [Jerard 2006a, Xu 2007]:

$$P_{avg} = K_{tc} \cdot \dot{Q} + K_{te} \dot{A}_c \quad (2)$$

where \dot{Q} is the material removal rate and \dot{A}_c is the contact area rate, both of which are determined by the cutting conditions and can be pre-calculated for each tool move in the CNC program [Jerard 06]. The average tangential force as a function of the power is:

$$F_{t_{avg}} = \frac{P_{avg}}{\omega \cdot r} \cdot \frac{2\pi}{\phi_{eng}} \quad (3)$$

where ω is the angular velocity, r is the tool radius and ϕ_{eng} is the angle of engagement of the cutter. The average chip thickness can be determined from the geometry of the cut as:

$$h_{avg} = \frac{1}{\phi_{eng}} \int_{\phi_{ent}}^{\phi_{ext}} f_t \cdot \sin(\phi) \cdot d\phi \quad (4)$$

where f_t is the feed per tooth.

Thus, the average tangential force as a function of the average chip thickness can be calculated from Equations (2), (3) and (4):

$$\frac{F_t}{a} = \frac{P_{avg}}{\dot{A}_c} = K_{tc} \cdot h_{avg} + K_{te} \quad (5)$$

where a is the axial depth of cut.

To calibrate the model, the average tangential force per axial depth is calculated from Equation 5 and plotted vs. the average chip thickness calculated with Equation 4. **Figure 4** illustrates how the coefficients of Equation 1 are found by obtaining the slope and intercept of the linear regression of data points obtained from a calibration test [Xu 2007].

Note that a slight change in slope may produce a large percent change in intercept. Small changes in the data often produces offsetting changes in the two coefficients. We have dubbed this the “see-saw” effect, an attribute of the coefficients that slightly complicates using them to track wear.

More information about calibration procedures to estimate the coefficients K_{TC} and K_{TE} are available in [Jerard 2006, Xu 2007, Desfosses 2007, 2008].

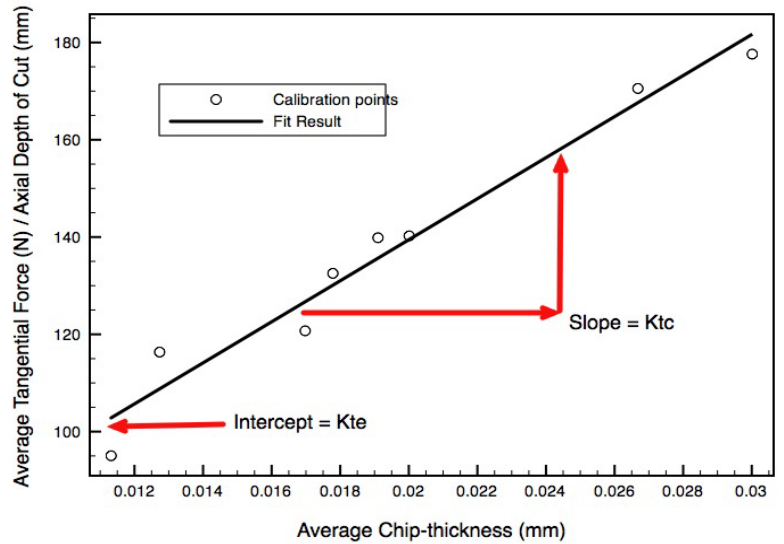


FIGURE 4: Least squares calibration of the tangential force model.

3. Sensors

In order for a tool condition monitoring system to be widely accepted by industry, the deployment onto shop floor machinery must be low cost, noninvasive, and cause no disruption of the machining envelope.

However, a monitoring system typically requires data collection sensors to be located on the machine. Unfortunately, many sensor types are high in cost, size, or are difficult to deploy. As a result, it is desirable for a monitoring system to take advantage of existing hardware infrastructure while using inexpensive sensors that have a low profile within the machine.

One instance of a non-invasive sensor is a power monitor located on a spindle drive motor [Schuyler 2006]. In this work, an example of combining mechanistic and geometric models with a spindle drive power monitor was discussed for end milling. Although non-invasive and cost effective, data sources such as power monitoring do not provide sufficient bandwidth to capture many important details of the machining process. During operations such as end milling, it is necessary to capture a broad range of frequencies for analysis purposes. Currently, this can be achieved with a variety of sensor types including force dynamometers, accelerometers, acoustic emissions sensors, or contact microphones.

A recent example can be seen in work by [Byrne et al., 07] for drilling and [Park 06] for end milling. In these studies, piezoelectric force sensors are integrated into the machine spindle. Although such devices are effective, machine tool manufacturers have yet to add sensor components to their products. From an industrial perspective, this is understandable. First, one can note the wide variety of sensor and signal processing combinations available [Rehorn 2004]. Often, each technique is coupled with a specific sensor type and is designed to solve a particular condition monitoring problem. From a research perspective, these sensor types are necessary for the development and validation of robust system models.

The sensing approach should accommodate cost, ease of setup, and performance. In order to meet these criteria, a sensor is proposed that utilizes existing hardware systems, does not require complex DAQ configuration, and has bandwidth comparable to a piezoelectric accelerometer. Additionally, this sensor is composed of common components that can be acquired at extremely low cost.

3.1 Electret Condenser sensor - We have been investigating an inexpensive alternative to traditional accelerometer and DAQ components for machine condition monitoring. We explore the feasibility of using a PC sound card for high bandwidth data acquisition from an epoxy-sealed electret condenser. This sensor's frequency response is contrasted against that of a commercial piezoelectric accelerometer amplified and sampled by a traditional DAQ system.

An electret condenser responds to vibration input by changing its capacitance. The electret used for this study is a Hosiden # KUB2823 and is characteristic of a commercially available electret condenser. This particular electret employs a diaphragm and is similar to the design detailed in [Sessler 1966]. The retail electret sensor components are, together, \$1.10 USD in cost, which makes the electret accelerometer an attractive alternative to a piezoelectric sensor if the appropriate response characteristics are possible.

3.2 Testing Procedure: A single-axis PCB piezoelectric accelerometer (Model 320 C33, serial number 5901) is fixed to a shaker table at the same reference point as the electret sensor. The output sensitivity of this piezoelectric accelerometer is 100mV/g. The PCB accelerometer has a known response and provides the baseline from which the electret sensor is benchmarked. Consequently, the specific response of the shaker table system is not of interest, since the piezoelectric accelerometer acts as the reference signal.

Tests were run to identify the lower limit of the sensor's response reliability. As with the Piezoelectric accelerometer, this limit occurs between 0 and 100 Hz. **Figure 5** details the 100 to 500 Hz range for both the piezoelectric and electret sensor indicating very similar response in that region..

The piezoelectric accelerometer bandwidth is from 1 to 4000 Hz ($\pm 5\%$). Since this sensor acts as the baseline for benchmarking the electret accelerometer, the spectra are evaluated over the range from zero to - 5000 Hz .

3.3 Results: The response of the electret accelerometer retained the same characteristics over multiple amplitude inputs. Therefore, the gain at any particular frequency is constant with respect to input amplitude. Consequently, at any particular input gain level, there exists a ratio spectrum between the outputs of the electret and piezoelectric accelerometers and is shown in **Figure 6**.

An electret accelerometer combined with sound card data acquisition is shown to be capable of replicating the response from a piezoelectric accelerometer and a traditional DAQ setup. Although the response of the electret accelerometer is not natively flat, it is a linear function of input amplitude from 1.3 to 6.6 g's. As a result, frequency deconvolution enables the electret accelerometer to perform closely to its piezoelectric counterpart. Considering that the electret accelerometer cost \$1.10 USD, the performance to cost ratio for this

sensor makes it an attractive alternative to the piezoelectric sensor for many applications.

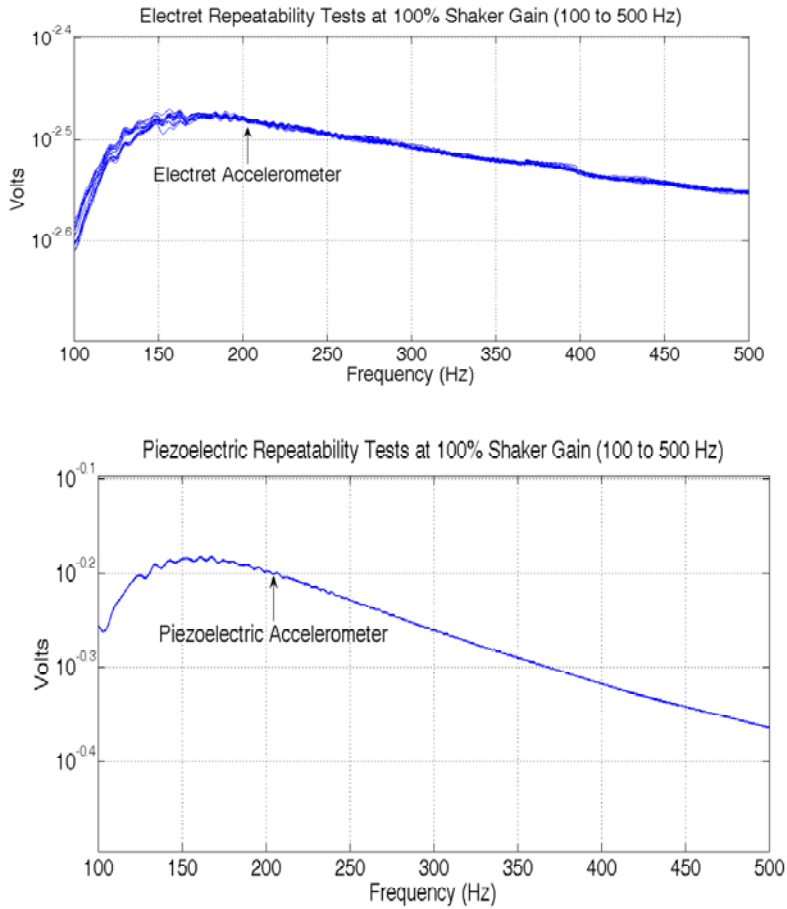


Figure 5 Detail of 0 to 500hz repeatability tests

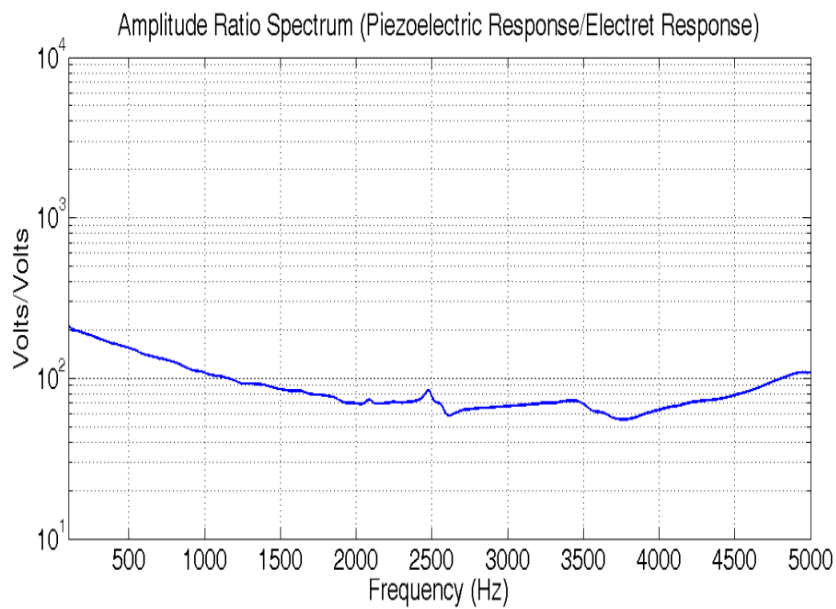


Figure 6 Amplitude Spectrum Ratio

4. Model Coefficient Variability

Statistical Study of Model Accuracy: Every model contains a certain degree of error and the force model of **Equation 1** is no exception. In particular, as shown in **Figure 2** the model coefficients, K_{tc} and K_{te} can change dramatically as the tool wears. The coefficients can also exhibit error as a function of the type of cutting conditions, changes in the material properties for the same nominal material, variations in the tool properties for the same nominal tool, tool material, tool coating, etc. Since we are attempting to use the coefficients to estimate forces it is important to know, in a statistical sense, the error associated with the model.

We have performed close to three thousand tests while varying the cutting conditions, average chip thickness, workpiece material, tool material and spindle speed. An example of our results, shown in **Figure 7**, illustrates the average maximum percent error for eight different cutting conditions. A 12.7 mm flat end cutter was used to make eight cuts of varying radial depth at four different feedrates using the average of 10 tests for each cutting condition. Power was measured for each cut and a regression was used to estimate K_{tc} and K_{te} .

As shown the Figure, the model is consistently underestimating power, and therefore forces, for the slot cutting conditions by an average of 3.63%. Center cutting, i.e. cutting which takes place primarily in the

center of the tool consistently overestimates power by an average of 1.2 percent.

These results help us to quantify the accuracy of the power and force estimates of the model when cutting conditions vary. It is not essential that the model be always 100% accurate as long as the uncertainty can be quantified. For example, when using the model to set safe feedrates based on the magnitude of the cutting force we can set a factor of safety that reflects the accuracy of the model. Further studies are being conducted to help quantify the effects of tool, workpiece and spindle speed variability. It was also quite helpful in streamlining our testing procedure as we discovered that running a single set of tests at 1/2 Down conditions yielded a set of coefficients almost as accurate as when using all eight conditions.



Figure 7 Shows the Maximum and average full scale percent error for eight different cutting conditions. The errors are maximum and average for four different feedrates for each of the eight cutting conditions using the average value of ten samples per condition.

5. Tool Wear: Figure 8 illustrates how the spindle motor power changes from cut to cut and over the life of a carbide cutter. The data points are for a slot cut followed by three down mills (75%, 50%, and 25% radial immersion). Power data was taken at five feed rates ranging from 81.5-128.0 mm/min. Figure 8 shows that the variation in power due to changing cutting conditions can far exceed the change caused by wear. Therefore, a wear estimation system based solely on power must compare identical cuts for power ratio or limit setting.

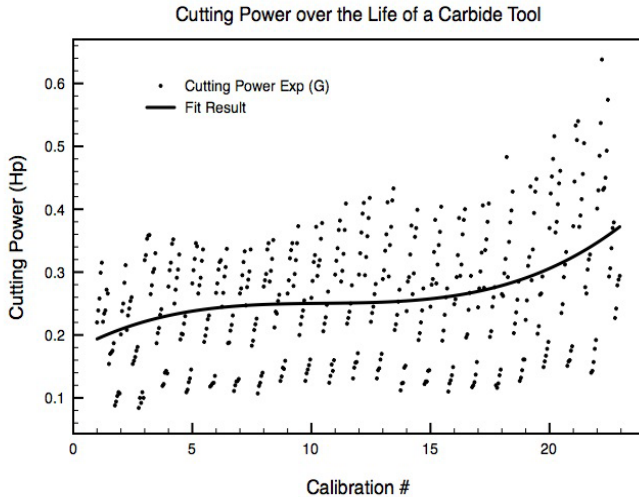


FIGURE 8: CUTTING POWER (HP) OVER THE LIFE OF A CARBIDE TOOL

In this research we use the coefficients of a tangential cutting force model to estimate the tool wear state. The model is calibrated by measuring spindle motor power over a variety of cutting geometries. We also show how

the pattern of the coefficients can be correlated with the type of wear, and we determine when a tool is worn out by a combination of the model coefficients.

Figure 9 shows cutting power versus time for four different values of average chip thickness. Figure 10 shows the corresponding micrographs of the tool edge. These tests were conducted by varying the feedrate to four different levels during each calibration so that the tool condition is approximately the same for each feedrate. At any given time, the power versus average feedrate can be plotted thereby defining the coefficients of Equation 5 as was previously shown in Figure 4.

If the power levels remain relatively equidistant from each other over time while gradually increasing this is reflected in an increase in K_{te} (edge or rubbing coefficient) with K_{tc} remaining roughly constant. On the other hand if the power levels begin to spread out over time this is reflected in an increase in the slope of the line shown in Figure 4, thereby indicating that the power levels are a function of chip thickness.

Figure 11 is a plot of the coefficients versus time for the test results shown in Figures 9 and 10. Generally, increasing values of K_{te} with time can be correlated with the amount of flank wear. Tool chipping often correlates with an increase in K_{tc} and a decrease in K_{te} .

By separating the cutting power into those components which are related to rubbing and those which are related to the shearing of the material we are able to classify the power changes while also providing information about the nature of the tool wear.

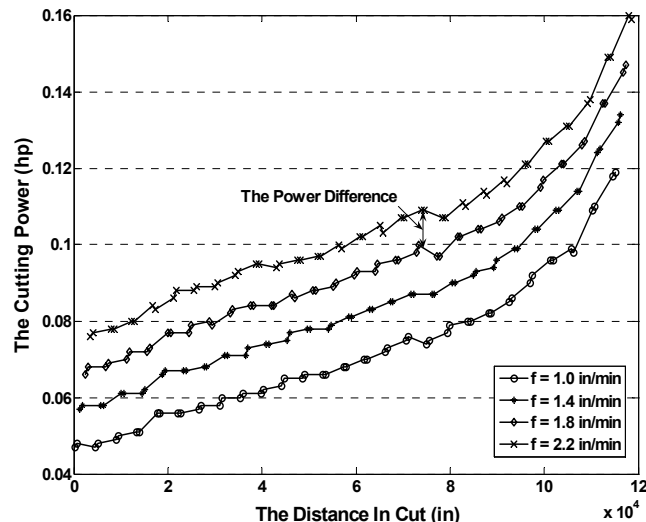


FIGURE 9: Cutting power increase with wear

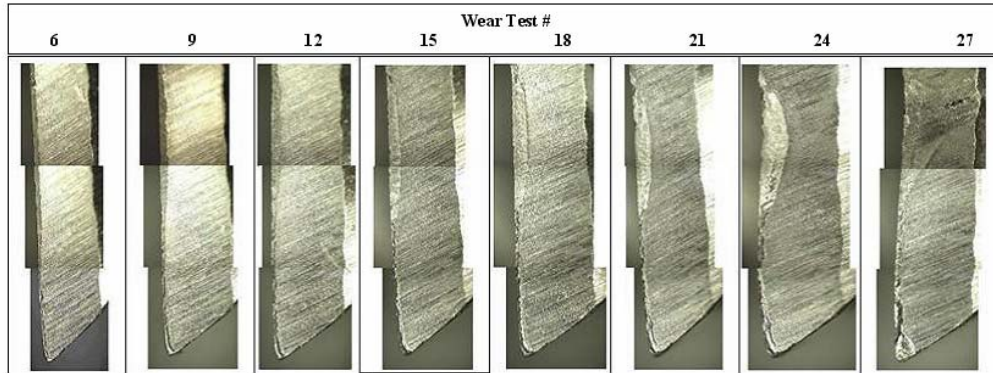


Figure 10 Micrographs of cutting edges at different stages of wear for the experiment shown in Figures 9 and 11.

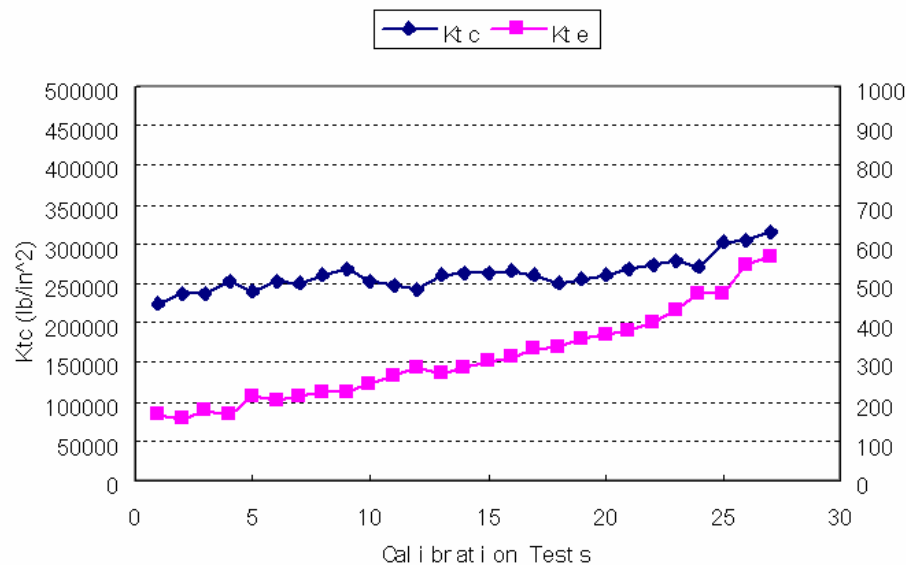


Figure 11 Tangential Force Model Coefficients as a function of time for the experiment shown in Figures 9 and 10.

5.1 Defining a worn tool: Some researchers define a tool to be completely worn when $VB = 0.6-0.8$ mm. However, the definition of a worn tool is highly dependent on the task the tool is performing. For roughing the tool can be used right up until the point of total failure, although it is important to change a tool before it breaks or melts to avoid damage to the part or the spindle bearings. For finish machining where surface finish is critical a much lower VB is acceptable.

5.2 Tool Wear Experiments and Setup: A number of experiments were performed to test the hypothesis that tangential force model coefficients are a reliable indicator of tool wear [ref NAMRC submission]. Most of the experiments were conducted with one-flute

cutters in order to eliminate the effects of runout and the need to average tool wear between multiple flutes. **Table 1** describes the experimental conditions. (Tables are the end of the paper).

An important observation about monitoring power can be seen in **Figure 12** which compares the results for Experiments G and H. These tests were performed in 1018 steel with 7.94 mm HSS cutters. The only difference between tests is the spindle speed. One might expect the two tests to have similar percent increases of power from the first cut to the last, but the 2444 rpm cut shows a 200% increase in power before the tool is completely worn out while the 3666 rpm case only reached about 100% increase in power for the

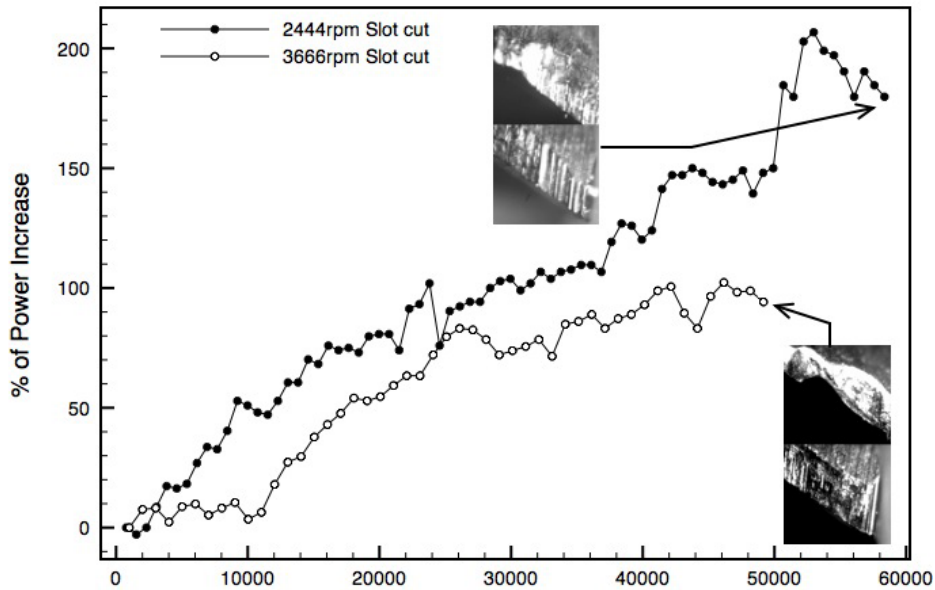


FIGURE 12: PERCENT POWER INCREASE VS. DISTANCE IN CUT (HSS SLOT CUTS IN 1018 STEEL EXPERIMENTS (G) AND (H))

same state of wear. The more aggressive cutting of Experiment (H) resulted in more chipping and a smaller percent increase in power.

The observation that nearly identical cutting conditions can result in very different percent increases in cutting power correlates with one of our primary conclusions, namely that the percent increase in cutting power at the end of usable tool life is dependent on the type of wear experienced by the tool. The difference between the two tests was that the 3666 rpm cut experienced some chipping along with flank wear. This chipping reduced the amount of flank wear land available for rubbing thereby reducing the final percent

power increase for the identical cuts.

From this observation it can be concluded that using a percentage power increase to assess tool condition is only viable if both the cutting conditions and the tool failure mode are identical. This imposes a severe limitation on commercial TCM systems. If any process variables are changed, e.g. spindle speed, tool material, tool coating, then it becomes necessary to retrain the system. These observations confirm the results reported by Pickett [Prickett 1999] who noted that the thresholds are a function of cutting conditions.

5.3 Results: In this section, the results of a typical experiment listed in Table 1 are presented and discussed. It should be noted that all the results are limited to helical end mills cutting 1018 steel and may not be consistent with other types of cutters and/or other materials. Changes in cutter geometry, e.g. tools with negative rake angles may also change the behavior of the coefficients as the tool wears. Additional testing needs to be conducted to see if consistent results can be obtained with other combinations of tools and materials.

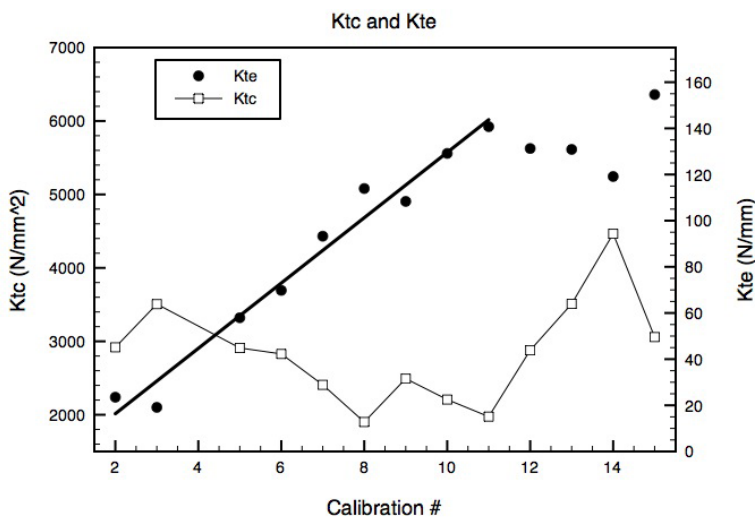


FIGURE 13: CALIBRATION COEFFICIENTS FOR A SMALLER DIAMETER CUTTER (9.525 mm HSS CUTTER IN 1018 STEEL, EXPERIMENT (E)).

Figure 13 shows results for Experiment (E). The coefficients for a smaller diameter cutter show very similar patterns to the coefficients of Experiment (A). K_{TE} is very linear until the end of tool life, at which point K_{TC} starts to increase. This correlates well with micrographs of the cutting edge presented in **Table 1** which show that the tool wear mode is flank wear.

5.4 Estimating Wear: A primary goal of this research is to find a method for indirectly measuring the percentage of tool life that has been expended. One significant finding that has been repeatedly shown throughout this investigation is that when flank wear is not the dominant mode the percent power increases are lower and a power based TCM system may experience difficulty. A second important finding is that the percent power increase at fully “worn out” condition is dependent on the average chip thickness and therefore a conventional TCM system must set different thresholds for different cutting conditions. We have also have seen that the model coefficients behave differently based on the mix of flank and non-flank wear on the tool edge. Our current research is focused on developing reliable correlations between the coefficients and the type and extent of tool damage.

6. Force Estimation using Feed Drive Power: While tangential force provides sufficient information for wear prediction, radial force information would likely increase the sensitivity and accuracy of the predictions. The spindle power can only provide tangential information; however, the feed drive motor power can provide average x and y cutting forces that can be used to determine the radial force model coefficients.

Current research is focused on estimating the average x cutting force from a load power sensor placed on the x-axis drive motor. Direct force measurement techniques, such as dynamometers, can be very fast and accurate, but the price and intrusiveness of these sensors severely limits their use. Although slower and less accurate than a dynamometer, indirect force measurement can be more practical for widespread implementation. The indirect measuring technique described in this section requires the installation of an electrical power sensor on the feed drive motor of a milling machine. In theory, the electrical power (or current) drawn by the electro/mechanical servo motor is related to the load felt by that motor. The tool/workpiece force, as reflected through the ball screw, is a component of that load.

The mechanical power (P_m) provided by the motor is used to overcome friction (P_f) and cut the part (P_{C-Ave}). The motor efficiency (η_e) relates the electrical power of the motor, to the mechanical output power:

$$P_m = \eta_e P_e = P_{C-ave} + P_f \quad (6)$$

The frictional power is estimated by measuring the tare power (P_t) without cutting. The actual cutting power can then be represented as:

$$P_{C-ave} = \eta_e P_e - \eta_e P_t \quad (7)$$

Once the motor is warmed up, tare power depends on the slide velocity and the position of the slide table in the machine workspace. Often, a machine has multiple slide covers that extend at certain locations of the table. For our machine, a Fadal EMC, the slide begins to extend at 100 mm, greatly increasing the tare power. All of our testing was performed within 100 mm to eliminate the sudden jump in P_t . If slide position is monitored the change in tare power can included in the calculation for P_{C-Ave} .

6.1 Experiment Setup: The machine used for this paper is a Fadal EMC mill. This is a three axis vertical mill. Each axis has a feed system driven by a three-phase AC brushless motor. A power sensor has been mounted on the x-axis feed drive motor. The sensor has an operational sensitivity of 0.01875 HP/V. The Fadal mill is also equipped with a Kistler dynamometer which is mounted directly under the workpiece. This directly measures the forces experienced by the workpiece in the x, y, and z directions.

The mechanical components of the feed system include the ball screw, table, lubricated table guides, and slide cover. These components create friction and damping that contribute to the tare power.

Forces are generated on the workpiece by a series of slot cuts. They were made with a 6 flute, 1/2” diameter, HSS end mill with a 30° helix angle. The workpiece material was 6061 aluminum. The spindle speed was set at 2653 rpm, and the feedrate set at 50 in/min in the x-direction. Each cut was performed at a different axial depth-of-cut so that different forces were generated in each case.

A data point was acquired every 3 degrees of spindle rotation for 120 complete revolutions. Given the spindle speed of 2653 rpm, the sample rate was 5306 points per second for 3.39 seconds. The results show that this is long enough to measure the average power.

6.2 Results: The feed drive power sensor system must be calibrated by comparing the power sensor output to the dynamometer output. At first, four slot cuts were performed with a 1/2 inch diameter cutting tool with 6 teeth. The cutting conditions are shown in **Table 2**. The only difference between each operation is the axial depth of cut. This was changed in order to generate different cutting forces.

During a segment of each cutting procedure the dynamometer output and power sensor output were recorded. Before each cut the tare power of the motor

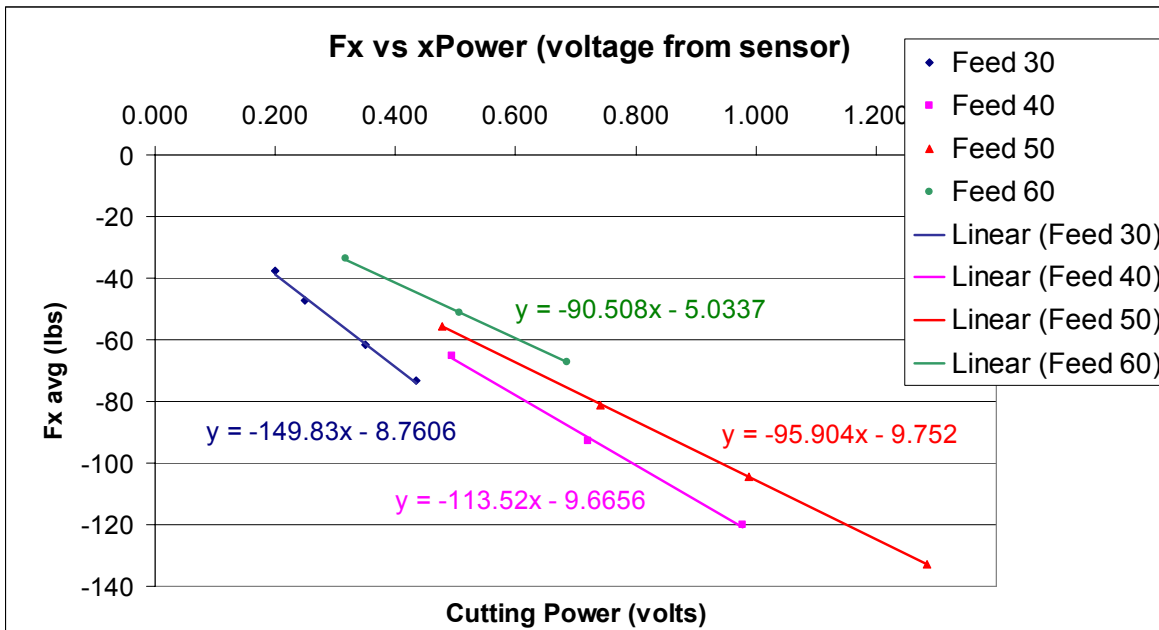


FIGURE 14: MEASURED CUTTING POWER, DETERMINED FROM THE SLIDE MOTOR POWER SENSOR, VS. MEASURED AVERAGE X-FORCE

was also measured during an equal-length segment before the tool entered the workpiece. Note that tare power is expected to be the same in each case since the conditions are identical.

Table 3 shows the total power measured by the feed drive power sensor during each cut as well as the tare power measured before each cut, the power due to the cutting force, and the cutting force measured by the dynamometer.

The average x-axis cutting force is plotted against the measured cutting power (sensor output voltage minus tare voltage) as shown in **Figure 14**. The data points at each feedrate fall on a straight line, indicating that steady state force can be accurately predicted from the power sensor for a given slide velocity. The slope of each of the lines is directly proportional to motor efficiency. A number of additional cutting tests at different slide velocities are necessary to generate an efficiency versus speed curve for the slide motor. Once the efficiency is known, the average x-force can be determined for any slide speed.

This investigation will continue by determining the accuracy limits under varying conditions. It is very likely the method could be used to calibrate the radial components of a force model if the cutting conditions are carefully controlled but it is less certain that the method will work under general cutting of a part.

7. Information Technology for Machine Tools: One of the advantages of using inexpensive, non-invasive sensors is that it is possible to collect vast quantities of data that can be used to perform model calibration, assess tool condition and the health of the machine tool. But a mountain of data is useless unless it can be organized into a database that provides structure, reliable archiving and integration with analysis routines. For example, an analysis tool could be developed to automatically extract machining history information from NCML files. Other file systems should be developed to store this extracted information (model parameters, tool life, etc.).

In many situations the data is never again used because either the particular experiment's exact setup has been forgotten or because the meaning of the data format has changed. No significant work has been done on this problem in the machining research field. In other fields, the Extensible Markup Language (XML) has successfully been used to facilitate data storage and exchange. For example, WellLogML was developed to hold well logs for the oil industry. Similarly in the medical field, ecgML was developed to hold electrocardiogram data. While neither of these solutions can be applied directly to sensor data for machining, the principals and ideas that they are based on can be reused to create a machining sensor data storage format.

7.1 IT Requirements: To be useful, a data format needs to be able to describe its contents explicitly and have the ability to change the format without invalidating older documents. Additionally, it should contain as much information as possible about the experiment, so that the contents can remain useful after the specifics have been forgotten by the experimenters.

It was decided to use XML for the basis of the new file format because it can describe its contents explicitly and allows changes to the format that won't render older files useless. Additionally, many libraries already exist for reading and writing XML compliant documents which saves considerable programming time when writing analysis tools. Using XML as the basis for the file format could help with other problems as well, such as the organization of data and information sharing between research groups.

XML is a markup language. Because XML only defines the structure of a file, an additional component called a schema is necessary to convey semantics or the "grammar" of the file. For example, nothing is wrong from an XML standpoint when a measurement has ten start times, but the schema tells the reader of a file that a measurement needs to have one and only one associated start time or it's not valid.

7.2 Methods: The basic representation of the hierarchy defined by the schema is exhibited in **Figure**

15. The root element of the XML file format is `experimentResults`. Every file needs one of these to be valid. It doesn't carry any real information, but is instead a container for everything else.

The `personnel` node is the first node in `experimentResults`. It holds information about the experimenter(s) that performed the measurements contained within the file. It needs at least one experimenter, but there is no upper limit.

`Configuration` is the second node. It holds things that don't change between individual measurements, like details about the machine (e.g. manufacturer and model number) work piece and purpose of the experiment. The schema doesn't specify the contents of this node, as the internals will vary between research groups.

Finally, there are an unlimited number of measurement nodes (at least one is required) inside `experimentResults`. The measurement nodes hold two configuration nodes called `startState` and `endState` for information about the experiment specific to that measurement (e.g. feed rate and G-Code line number). Anything that changes in an unpredictable manner between the start and end of a measurement should probably be modeled as a sensor instead of a configuration entry.

Each measurement can house any number of interface

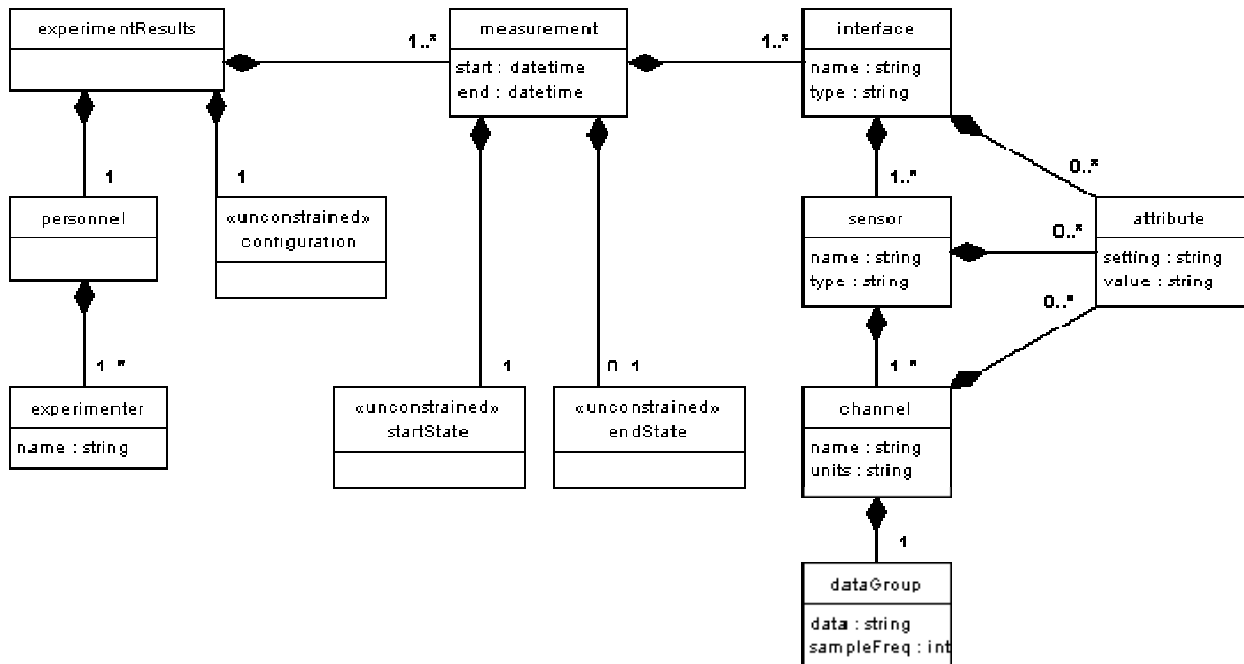


FIGURE 15: SCHEMA HIERARCHY OF XML DATA FILE

nodes. Interface nodes represent the physical interface between the computer and sensors, such as an A/D board or a sound card. Interfaces house sensors which in turn house channels. Channel nodes hold the dataGroup nodes, where the actual measurements are stored. While most sensor nodes will only have one channel, it is advantageous to allow for cases where a single sensor represents many streams of incoming data (e.g. a three axis force sensor).

7.3 Implementation: Several tools were written in MATLAB to take advantage of the ability to read both sensor data and experiment configuration from the same file. The most basic of these tools is the Fourier analysis tool designed to show a time trace and frequency spectrum on the same plot (see **Figure 16**).

Because XML is such a prevalent format and because robust libraries are widespread, storing measured results into the new data format was relatively painless. Similarly, writing new analysis tools in MATLAB is straight forward as MATLAB already supports reading XML files. The format accomplishes the requirements set for it, with an explicit description of the file, extensibility, and housing configuration and measurement data in the same file.

7.3 Information Sharing: Information sharing between research groups at different organizations is a related problem. Currently, there is no standardized format for the exchange of machining sensor data. The XML schema that has been developed would not solve the problem because the schema doesn't specify exactly what the contents of the configuration sections are (because different research groups have different needs). It would, however, simplify the problem because XML already provides a way to transform file contents from one schema to another. It does this through the XSLT language. Further investigation will be required to determine the best way to utilize this functionality.

Organizing machining data presents yet another problem. Storing the data on a computer file system with hierarchical directories is the simplest approach, but it can be troublesome to search for a specific experiment without knowing exactly where in the directory structure it is located. Manual indexing schemes are possible, but prone to error because the system is not automated. Using native XML databases to house the machining data is one promising option.

Native XML databases store files in such a way that the data can quickly be retrieved by searching for

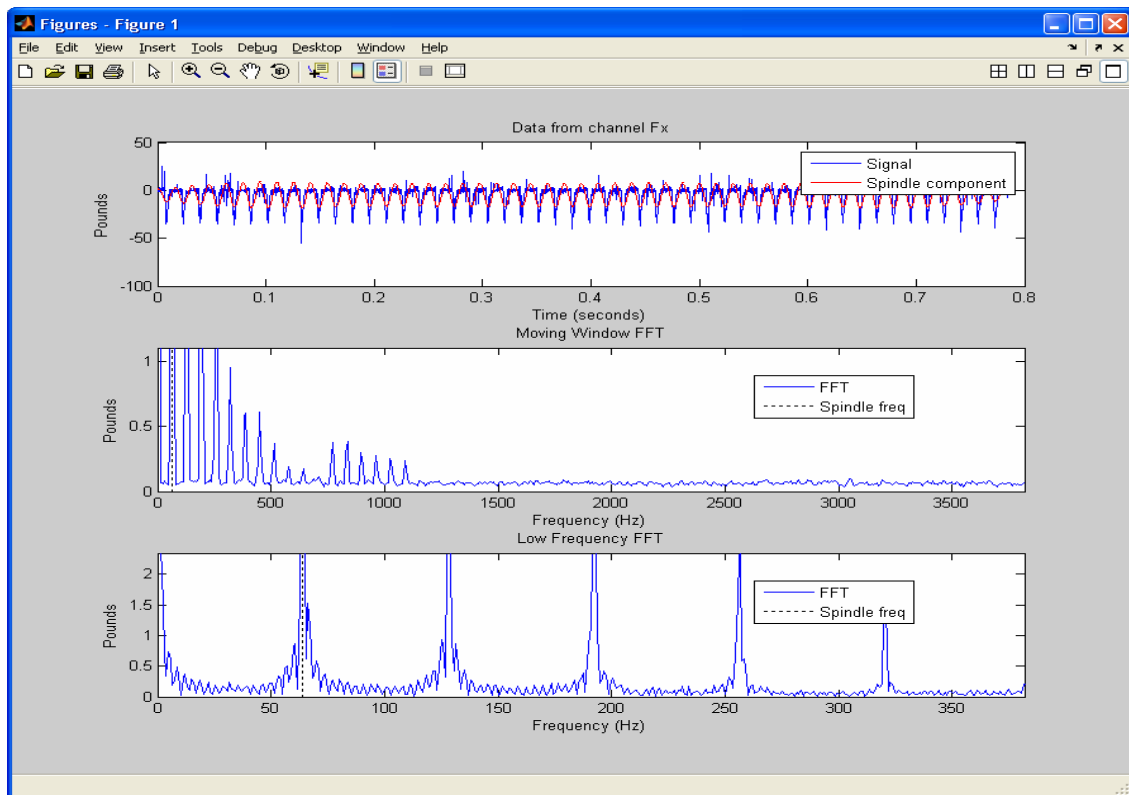


FIGURE 16: MATLAB BASED FOURIER ANALYSIS TOOL

portions of the file. While native XML databases are not as mature as SQL databases, they are becoming more widespread for data already in an XML form. They show great promise for situations where the search terms of interest aren't known at the time of database creation, as they can search through the entire contents of the file, something that other databases aren't geared toward.

9. Summary: This paper summarizes recent progress in the development of Smart Machining Systems at the University of New Hampshire. Our approach is based on the integration of models of the machining process, the use of low cost non-invasive sensors and Information Technology to archive and retrieve the data.

Future work will continue to focus on each of the areas described in this paper. In particular, we need to add both models and sensor that will capture the effects of machine dynamics, e.g. chatter conditions.



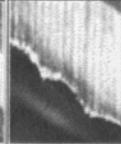




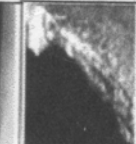
6. Acknowledgements The support of the National Science Foundation under grants DMI-0322869 and DMI-0620996 is gratefully acknowledged. We also thank Marian Noronha, President of TurboCam of Dover, NH for his assistance in providing test cases.

7. References

- [Altintas 2000] Altintas, Y., Manufacturing Automation: Metal Cutting Mechanics, Machine Tool Mechanics, Machine Tool Vibrations, and CNC Design, Cambridge University Press, ISBN 0-521-65973-6.
- [Byrne 2007] Byrne, G. and G.E O'Donnell "An Integrated Force Sensor Solution for Process Monitoring of Drilling Operations." *CIRP Annals-Manufacturing Technology*, Vol. 56, Issue 1, pp.89-92.
- [Desfosses 2007] Desfosses, B., An Improved Power Threshold Method for Estimating Tool Wear During Milling, MS Thesis, Dept. of Mechanical Engineering, The University of New Hampshire.
- [Desfosses 2008] Desfosses, B., R.B. Jerard, B.K. Fussell and M. Xu, "An Improved Power Threshold Method for Estimating Tool Wear During Milling", Submitted to 36th Annual North American Manufacturing Research Conference, May 20-23, Monterrey, Mexico.
- [Jacobson 2006] Jacobson, D, B.K. Fussell and R.B. Jerard, "Tool Runout Estimation Using Feed Force Spectral Components", presented at the 2006 ASME International Conference on Manufacturing Science and Engineering, Oct 8-11, Ypsilanti, MI.
- [Jerard 2006a] Jerard, R. B., B. K. Fussell, M. Xu, C. Yalcin, Process Simulation and Feedrate Selection for Three-axis Sculptured Surface Machining, *International Journal of Manufacturing Research*, 1(2), pp. 136-156.
- [Jerard 2006b] R B. Jerard, Okhyun Ryou, "NCML: a data exchange format for internet-based machining," *International Journal of Computer Applications in Technology (IJCAT)*, Vol. 26, No. 1/2, p. 75-82
- [Jerard 2007a] Robert B. Jerard, Barry K. Fussell, Min Xu, Chad Schuyler, A Testbed for Research on Smart Machine Tools, poster presentation at the International Conference on Smart Machining Systems, NIST, Gaithersburg, MD, March 13-15.
- [Jerard 2007b] Robert B. Jerard, Min Xu, Barry K. Fussell, Cutting Power Model-Sensor Integration for Tool Condition Monitoring, presented at The International Conference on Smart Machining Systems, NIST, Gaithersburg, MD, March 13-15.
- [Jerard 2007c] Robert B. Jerard, NCML: An XML Based NC Programming Language, presented at The International Conference on Smart Machining Systems, NIST, Gaithersburg, MD, March 13-15.
- [Park 2006] Park, S.S.. "Identification of Spindle Integrated Force Sensor's Transfer Function for Modular End Mills." *Journal of Manufacturing Science and Engineering*, Vol. 128, Issue 1, pp. 146-153.
- [Prickett 1999] Prickett, P. W. and C. Johns, "An overview of approaches to end milling tool monitoring", *International Journal of Machine Tools and Manufacture*, Vol. 39, pp. 105-122.
- [Rehorn 2004] Rehorn, A. G., J. Jiangand, and P. E. Orban, "State-of-the-art methods and results in tool condition monitoring: a review," *International Journal of Advanced Manufacturing Technology*, DOI 10.1007/s00170-004-2038-2.
- [Saturley 2000] Saturley, P. V. and A.D. Spence, "Integration of Milling Process Simulation with On-Line Monitoring and Control", *Int J Adv Manuf Technol* (2000) 16: pp. 92-99
- [Schuyler 2006] Schuyler, C.K., M. Xu, R.B. Jerard and B.K. Fussell, "Cutting power model-sensor integration for a smart machining system," *Transactions of the North American Manufacturing Research Institution/SME Volume 34, NAMRC 34, Marquette University, May 23-26.*
- [Sessler 1966] Sessler, G.M. and J.E. West, "Foil-Electret Microphones." *The Journal of the Acoustical Society of America*, Vol. 40, Issue 6, pp. 1433-1440.
- [Suprock 2008] Suprock, C.A., B.K. Fussell, R.B. Jerard and J.T. Roth, "A Cost Effective Accelerometer and DAQ for Machine Condition Monitoring: A Feasibility Study," Submitted to 36th Annual North American Manufacturing

- Research Conference, May 20-23, Monterrey, Mexico.
- [Xu 2006a] Xu, Min, C. K. Schuyler, B. K. Fussell, R. B. Jerard, "Experimental Evaluation Of A Smart Machining System For Feedrate Selection And Tool Condition Monitoring", Transactions of the North American Manufacturing Research Institution/SME (NAMRC) Volume 34, Marquette University, May 23-26.
- [Xu 2006b] Xu, Min, C. K. Schuyler, B. K. Fussell, R. B. Jerard, Patent Provision Application, Method to Measure Tool Wear from Process Model Parameters, Filed on 12/2/2006
- [Xu 2007] Xu, Min, Robert B. Jerard and Barry K. Fussell, (2007), Energy Based Cutting Force Model Calibration for Milling, Comput.-Aided Des. Appl., Vol. 4, Nos. 1-4, p 341-351.
- [Zhu 2003] Zhu, R., R.E. DeVor. and S.G. Kapoor, "A Model-Based Monitoring and Fault Diagnosis Methodology for Free-Form Surface Machining Process", ASME J. of Manuf. Sci. and Eng., August 2003, Vol. 125, pp. 397-404. Min Xu, Robert B. Jerard, Barry K. Fussell, (2007), Energy Based Cutting Force Model Calibration for Milling, Comput.-Aided Des. Appl., Vol. 4, Nos. 1-4, p 341-351.

TABLE 1: DETAILS OF THE TOOL WEAR EXPERIMENTS

Experiments								
	A	B	C	D	E	F	G	H
Cutter Material	HSS	HSS	Carbide	Carbide	HSS	Carbide	HSS	HSS
Tool Diameter (mm)	12.7	12.7	12.7	12.7	9.525	9.525	7.9375	7.9375
Number of flutes	1	1	4	4	1	1	1	1
Spindle Speed (rpm)	1068	1528	2674	4011	1068	3055	2444	3666
Feed per tooth (mm)	.019 .028 .033 .040	.053	.076	.051	.019 .028 .033 .040	.027 .030 .034 .038 .041	.0254	.0254
Entrance/Exit angles (deg)	0/180 60/180 90/180 120/180	90/180	120/180	120/180	0/180 60/180 90/180 120/180	0/180 60/180 90/180 120/180	0/180	0/180
Dist between calib	0	.152	3.39	3.39	0	0	.610	.610
Dominant Wear Mode	FW	FW	CH	CH	FW	CH	FW	FW +
Photo of tool wear (30x)								

Notes:

1. 1018 Steel was the material used to wear out the tool in all experiments.
2. Experiments A, E and F experienced wear at all combinations of feed/tooth and entrance/exit angles; Calibration occurred continuously as the tool wore.
3. Experiments B, C, D, G and H were worn at constant conditions with periodic calibrations as indicated by the distance between calibrations. B, C, D were calibrated using 1018 steel; G, H were calibrated with a sacrificial block of aluminum.

TABLE 2: CUTTING CONDITIONS FOR MEASURING FEEDRIVE POWER

Cut #	Spindle Speed w (rpm)	SlotCut Feedrate, f (in/min)	havg (in)	Axial Depth a (in)
1	3183	30	0.0005	0.160
2	3183	30	0.0005	0.240
3	3183	30	0.0005	0.320
4	3183	30	0.0005	0.400
5	2122	40	0.0010	0.240
6	2122	40	0.0010	0.360
7	2122	40	0.0010	0.480
8	2653	50	0.0010	0.192
9	2653	50	0.0010	0.288
10	2653	50	0.0010	0.384
11	2653	50	0.0010	0.480
12	3183	60	0.0010	0.160
13	3183	60	0.0010	0.240
14	3183	60	0.0010	0.320

Table 3: POWER AND FORCE MEASUREMENTS FOR THE CUTTING CONDITIONS OF TABLE 2

Cut #	Feed	Total Power During Cut*	Tare Power Before Cut*	Power due to Cutting Force*	F _{x,avg} (lb)
1	30	0.014	0.010	0.004	-38
2	30	0.015	0.010	0.005	-47
3	30	0.016	0.010	0.007	-62
4	30	0.018	0.010	0.008	-73
5	40	0.021	0.012	0.009	-65
6	40	0.025	0.012	0.014	-93
7	40	0.030	0.012	0.018	-120
8	50	0.023	0.014	0.009	-55
9	50	0.027	0.013	0.014	-81
10	50	0.032	0.014	0.019	-104
11	50	0.038	0.014	0.024	-133
12	60	0.024	0.018	0.006	-34
13	60	0.028	0.018	0.009	-51
14	60	0.031	0.018	0.013	-67

*Output of power sensor is in volts. Volts can be related to horsepower by the operational sensitivity of the power sensor (0.01875 HP/Volt).